

基于气动弹性剪裁的风力机叶片模态分析

陈文朴, 李春叶, 舟繆维跑

(上海理工大学能源与动力工程学院, 上海 200093)

摘要: 本文为研究叶片铺层参数对叶片动态特性的影响, 防止叶片产生共振, 改善叶片力学特性, 建立了1.5 MW风力机叶片的有限元模型, 通过改变铺层角度和铺层纤维比例实现多种不同层合板结构的叶片铺层, 并对上述各种铺层叶片结构进行了模态分析, 获得了各模型的前六阶固有频率和振型, 分析了铺层参数影响叶片动态特性的原因。结果表明: 复合材料具有显著各向异性, 通过改变铺层角度能影响固有频率大小; 叶片低阶振型以挥舞和摆振为主, 增加0°铺层比例能提高低阶固有频率; 叶片高阶模态出现扭转, 45°铺层能提高叶片抗扭能力, 有利于增加高阶固有频率。

关键词: 风力机; 叶片; 气动弹性剪裁; 模态

中图分类号: TK83 文献标识码: A

DOI: 10.16146/j.cnki.rndlgc.2016.09.009

引言

叶片是风力机的核心部件之一, 叶片的结构设计对整个风力机的安全运行起重要作用^[1]。随着风电机组不断大型化, 叶片尺寸和重量增加, 叶片结构设计需要满足更高的要求^[2]。叶片作为大型的细长弹性结构, 作用在叶片上的载荷包括空气动力、自身惯性力和弹性力等, 这些载荷具有交变性和随机性, 因此风力机运行过程中叶片必然发生振动^[3]。

因此叶片结构设计中首先需要满足强度和刚度的要求, 同时降低叶片振动, 避免共振产生, 叶片设计必须考虑其固有频率, 防止叶片自振频率与风轮转速频率重合^[4]。为了减轻叶片重量, 减小制造成本, 大型风力机叶片普遍采用玻璃纤维增强复合材料, 由于复合材料纤维与基体性能差异大, 沿纤维方向性能最佳, 复合材料具有显著地正交各向异

性^[5-7]。气动弹性剪裁正是利用复合材料极高的可设计性, 通过改变材料的刚度方向达到控制叶片结构的动静态气动弹性变形, 从而调整叶片固有频率。

针对此问题, 国内外许多学者开展了相关研究。Gangele 基于有限元法分析了不同材料对叶片固有频率的影响^[8], 但其简化了叶片铺层结构。Griffith 针对尺寸约为9 m的叶片实验获得了叶片的动态特性^[9], 但因其尺寸与大型风力机叶片相差较大, 无法准确反映大型风力机叶片的结构特性。文献[10~11]主要分析了铺层参数对叶片静态结构性能的影响, 并未研究其对叶片动态力学性能的影响。

本文在上述研究的基础上, 以NREL(国家可再生能源实验室)设计的1.5 MW风力机叶片为研究对象, 利用参数化建模建立多翼型叶片三维壳体模型, 改变叶片铺层角度实现气动弹性剪裁仿真, 通过模态分析获得铺层参数对叶片动力学特性的影响及其物理机制, 得出复合材料不同气动弹性剪裁方式对叶片结构影响的变化规律, 以此改善叶片结构特性。

1 有限元模态分析

叶片经有限元离散化处理后, 系统运动方程为^[12]:

$$M\ddot{u} + C\dot{u} + Ku = 0 \quad (1)$$

式中: M —结构的质量矩阵; C —结构的阻尼矩阵; K —结构的刚度矩阵; \ddot{u} —加速度矢量; \dot{u} —速度矢量; u —位移矢量。

若系统无外载荷, 方程的解反映了结构的固有频率及振型。工程上讨论叶片固有特性时通常忽略阻尼作用, 式(1)变为:

收稿日期: 2015-12-06; 修订日期: 2016-01-11

基金项目: 国家自然科学基金资助项目(51176129, 51176129, 51676131); 上海市教育委员会科研创新(重点)项目(No. 13ZZ120, 13YZ066); 教育部高等学校博士学科点专项科研基金(博导类)项目(20123120110008)

作者简介: 陈文朴(1991-), 男, 上海人, 上海理工大学硕士研究生。

$$M\ddot{u} + C\dot{u} + Ku = 0 \tag{2}$$

式(2)的解析式为:

$$u = X\sin\omega t \tag{3}$$

式中: X —模态形状; ω —固有频率, Hz; t —时间, s。

将式(3)带入式(2)得:

$$(K - \omega^2 M) X = 0 \tag{4}$$

令 $\lambda = \omega^2$, 则式(4)存在非零解的条件为:

$$\det(K - \lambda M) = 0 \tag{5}$$

式(5)为广义特征方程, 是 λ 的 n 次代数方程, 由此可得:

$$(K - \lambda_i M) X = 0 \quad i = 1, 2, \dots, n \tag{6}$$

求解特征方程式(6), 可求得模态形状 X 和固有频率 ω_i 。

2 层合板及叶片模型

2.1 层合板结构模型

风力机叶片铺层的基本形式是层合板, 如图 1 所示, 层合板是各单层板沿铺层厚度方向粘合而成的多层材料结构^[13], 其中单层板主要由两部分组成: (1) 纤维起承载作用; (2) 基体起粘结纤维和传递应力的作用。叶片铺层采用的复合材料具有各向异性, 其纤维方向(图中 x_1 方向)具有最大的抗拉强度, 垂直于纤维的方向(图中 y_1 方向)抗拉强度相对较差。单层板坐标系 ($x_1 - y_1 - z_1$) 与层压板总体坐标系 ($x - y - z$) 的关系如图 1(b) 所示。本文中层合板 x 轴与叶片展向(叶片 x 方向)一致称为纵向, 层合板 y 轴方向称为横向, 层合板 z 轴与单层板轴 z_1 方向一致为铺层厚度方向。各单层板轴 x_1 方向与 x 轴方向的偏角 θ 称为铺层角度。

2.2 叶片有限元模型

本文以某典型 1.5 MW 叶片作为研究对象, 叶片沿展向分为叶根、叶中和叶尖三部分, 为兼顾气动和结构性能, 分别采用 NREL 的 S818、S825 和 S826 翼型, 叶片长度为 33 m, 最大弦长为 2.72 m, 额定转速为 20 r/min, 额定风速为 8 m/s, 叶片有限元模型如图 2 所示。叶片根部需设置约束条件, 叶片以 Y 轴为旋转轴, 其余 5 个自由度为零。

叶片主要结构如图 3 所示, 图中 c 为弦长。叶片结构为主梁双腹板结构。图中①为腹板, 分为前

腹板和后腹板, 分别安装于弦长 15% 和 50% 两处位置。图中②为梁帽, 其安装于腹板之间。梁帽和腹板构成箱型主梁结构, 起主要承载作用。

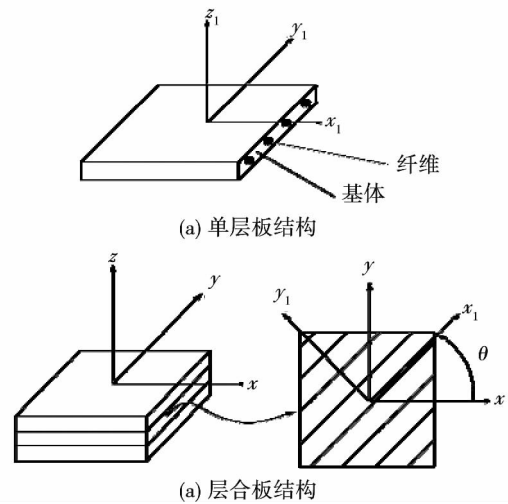


图 1 单层板和层合板结构示意图

Fig. 1 Schematic drawing of the structure of a single layer plate and ply plate

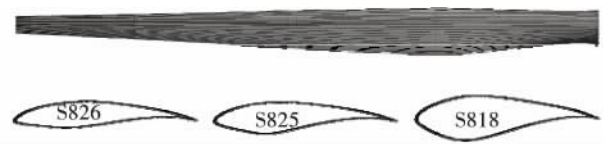


图 2 叶片有限元模型

Fig. 2 Finite element model for blades

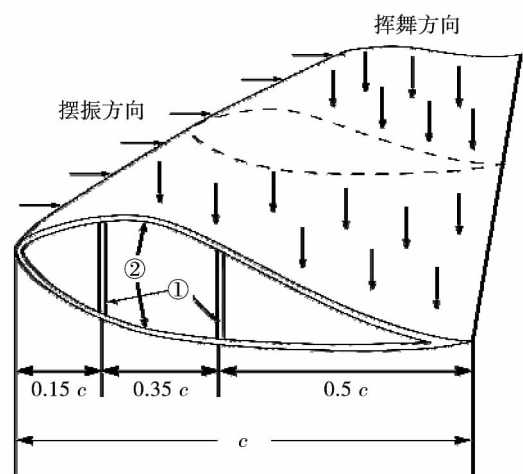


图 3 叶片结构示意图

Fig. 3 Schematic diagram of the structure of a blade

3 叶片材料及铺层结构

叶片材料应具有足够的强度、刚度和疲劳强度，此外还需考虑材料应具备质量轻、成型工艺简单以及材料来源丰富^[14]。结合以上因素，本文叶片的蒙皮、梁帽和腹板由胶衣、单向布、双向布和巴沙木组成。表 1 为叶片所用材料的力学特性， E_x 为纵向弹性模量， E_y 为横向弹性模量， ν_{xy} 为泊松比， G_{xy} 为剪切模量。

表 1 铺层材料力学特性

Tab. 1 Characteristics of the lamination material in mechanics

| 材料 | E_x /GPa | E_y /GPa | G_{xy} /GPa | ν_{xy} |
|-----|------------|------------|---------------|------------|
| 胶衣 | 3.44 | 3.44 | 1.38 | 0.3 |
| 单向布 | 31 | 7.38 | 3.52 | 0.28 |
| 双向布 | 10.3 | 10.3 | 8.0 | 0.3 |
| 巴沙木 | 2.07 | 2.07 | 0.14 | 0.22 |

叶片铺层厚度自叶根向叶尖方向逐渐减小，梁帽厚度先增加后减小。叶片表面和前后腹板均采用三明治夹心结构，结构两侧铺设单轴和双轴向玻璃纤维复合材料层合板，中间层以巴沙木为核心。胶衣铺设在叶片最外层表面，保护结构层材料不受外界环境介质侵蚀，叶片铺层结构如图 4 所示。

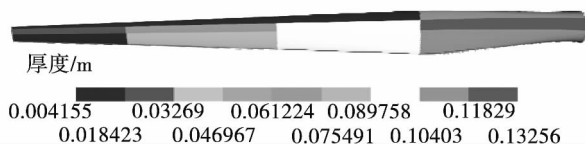


图 4 叶片铺层示意图

Fig. 4 Schematic diagram of the lamination layer on the blade

4 叶片模态特性分析

为了改善叶片动态特性，文献 [15 ~ 16] 的设计方法，通过改变铺层角度实现叶片的气动弹性剪裁，用以提高叶片的动态性能。叶片以巴沙木为夹芯材料，由于其密度较低，并能为叶片提供足够的刚度，但其为各向同性材料，并不具备很高的可设计性。

玻璃钢复合材料为各向异性材料，其纤维方向的力学性能远优于其它方向的性能，而风力机叶片载荷主要集中在一个方向，叶片展向是弯曲载荷的主要加载方向，因此通常复合材料纤维 0° 方向指向叶片展向，通过改变纤维方向与叶片展向夹角的角度，可以改变叶片的强度和刚度等结构特性。巴沙木两侧为双向布和单向布， $\pm 45^\circ$ 双向布用于梁帽和腹板结构，主要是为了抵抗叶片扭转产生的剪应力和在单向布间传递载荷。因此本文主要通过改变梁帽和蒙皮的玻璃纤维单向布与叶片展向的夹角角度实现气动弹性剪裁，以 15° 为间隔从 0° 变化到 90° ，通过模态分析，计算获得叶片前六阶固有频率。

为确保叶片结构计算结果可靠，必须首先保证叶片满足强度和刚度要求。文献 [17] 中实测了某 1.5 MW 风力机叶片在极限工况下，最大叶尖位移 8.12 m，叶片最大的允许拉伸和压缩强度分别为 720 和 380 MPa，改变铺层角度获得叶片最大的变形和拉压应力如表 2 所示，与实验结果对比，说明叶片在额定工况下能满足强度要求。

表 2 叶片变形和最大应力

Tab. 2 Blade deformation and maximum stress

| 铺层角度 / ($^\circ$) | 叶尖位移 / m | 拉应力 / MPa | 压应力 / MPa |
|---------------------|----------|-----------|-----------|
| 0 | 3.26 | 138 | 122 |
| 15 | 3.50 | 134 | 119 |
| 30 | 3.53 | 96 | 85 |
| 45 | 3.50 | 91 | 82 |
| 60 | 3.74 | 102 | 90 |
| 75 | 3.91 | 114 | 104 |
| 90 | 3.75 | 120 | 106 |

表 3 和表 4 分别为不同铺层角度下叶片挥舞和摆振方向各截面的刚度，文献 [18] 中技术文件提供了叶片各截面的刚度值，计算结果与文件所提供的的数据基本吻合，从而确保了叶片刚度能满足设计要求。

叶片通过模态分析确定其结构的固有频率和振型，在结构设计中它们是承受动态载荷的重要参数。由于共振是引起叶片结构破坏的重要原因，因此要求叶片的固有频率远离其旋转频率，防止风轮产生共振。

表 3 叶片挥舞刚度($N \cdot m^2$)
Tab. 3 Flapwise stiffness of the blade($N \cdot m^2$)

| 截面编号 | 0° | 15° | 30° | 45° | 60° | 75° | 90° | 技术文件值 |
|------|-----------------------|-----------------------|--------------------|--------------------|--------------------|--------------------|--------------------|--------------------|
| 1 | 1.17×10^{10} | 1.07×10^{10} | 8.27×10^9 | 6.36×10^9 | 5.66×10^9 | 5.43×10^9 | 5.36×10^9 | 6.27×10^9 |
| 2 | 2.77×10^9 | 2.50×10^9 | 1.86×10^9 | 1.36×10^9 | 1.17×10^9 | 1.16×10^9 | 1.17×10^9 | 8.71×10^8 |
| 3 | 1.24×10^9 | 1.10×10^9 | 7.74×10^8 | 5.16×10^8 | 4.22×10^8 | 4.26×10^8 | 4.26×10^8 | 4.73×10^8 |
| 4 | 7.95×10^8 | 7.06×10^8 | 4.85×10^8 | 3.12×10^8 | 2.49×10^8 | 2.65×10^8 | 2.66×10^8 | 1.49×10^8 |
| 5 | 1.79×10^8 | 1.58×10^8 | 1.09×10^8 | 7.01×10^7 | 5.59×10^7 | 5.90×10^7 | 5.91×10^7 | 5.36×10^7 |
| 6 | 9.63×10^7 | 8.55×10^7 | 5.88×10^7 | 3.78×10^7 | 3.02×10^7 | 3.17×10^7 | 3.18×10^7 | 2.16×10^7 |
| 7 | 4.72×10^7 | 4.19×10^7 | 2.88×10^7 | 1.86×10^7 | 1.48×10^7 | 1.55×10^7 | 1.55×10^6 | 7.40×10^6 |
| 8 | 2.06×10^7 | 1.83×10^7 | 1.27×10^7 | 8.23×10^6 | 6.62×10^6 | 7.06×10^6 | 7.06×10^6 | 2.68×10^6 |
| 9 | 1.30×10^7 | 1.15×10^7 | 7.98×10^6 | 5.20×10^6 | 4.19×10^6 | 4.48×10^6 | 4.45×10^5 | 4.73×10^5 |

表 4 叶片摆振刚度($N \cdot m^2$)
Tab. 4 Edgewise stiffness of the blade($N \cdot m^2$)

| 截面编号 | 0° | 15° | 30° | 45° | 60° | 75° | 90° | 技术文件值 |
|------|--------------------|--------------------|---------------------|--------------------|--------------------|--------------------|--------------------|--------------------|
| 1 | 7.06×10^9 | 6.85×10^9 | 6.31×10^9 | 5.83×10^9 | 5.64×10^9 | 5.59×10^9 | 5.55×10^9 | 6.27×10^9 |
| 2 | 2.77×10^9 | 2.61×10^9 | 2.20×10^9 | 1.84×10^9 | 1.69×10^9 | 1.86×10^9 | 2.27×10^9 | 1.73×10^9 |
| 3 | 2.20×10^9 | 2.07×10^9 | 1.75×10^9 | 1.46×10^8 | 1.34×10^8 | 1.48×10^8 | 1.81×10^9 | 1.51×10^8 |
| 4 | 1.72×10^9 | 1.62×10^9 | 1.36×10^9 | 1.14×10^9 | 1.05×10^9 | 1.15×10^9 | 1.41×10^9 | 6.45×10^8 |
| 5 | 1.31×10^9 | 1.23×10^9 | 1.04×10^9 | 8.67×10^8 | 7.98×10^8 | 8.79×10^8 | 1.07×10^9 | 2.70×10^8 |
| 6 | 9.70×10^8 | 9.14×10^8 | 7.69×10^8 | 6.43×10^8 | 5.91×10^8 | 6.51×10^8 | 7.96×10^8 | 1.30×10^8 |
| 7 | 5.08×10^8 | 4.78×10^8 | 4.02×10^8 | 3.36×10^8 | 3.09×10^8 | 3.41×10^8 | 4.17×10^8 | 6.19×10^7 |
| 8 | 3.48×10^8 | 3.28×10^8 | 2.76×10^8 | 2.30×10^8 | 2.12×10^8 | 2.33×10^8 | 2.85×10^8 | 2.75×10^7 |
| 9 | 2.34×10^8 | 2.20×10^8 | 1.855×10^8 | 1.55×10^8 | 1.42×10^8 | 1.56×10^8 | 1.91×10^8 | 6.56×10^6 |

由于能量主要集中于前几阶模态,高阶模态精度不足,因此在工程应用中,主要考虑前几阶模态,叶片 0°铺层方向的前六阶固有频率如图 4 所示,随着阶数增加,叶片固有频率逐渐增大。

表 5 0°铺层前六阶固有频率

Tab. 5 Natural frequency of blade with 0° ply angle

| 0° | 一阶 | 二阶 | 三阶 | 四阶 | 五阶 | 六阶 |
|------|------|------|------|------|------|------|
| 固有频率 | 0.84 | 1.25 | 2.46 | 4.58 | 5.67 | 8.87 |

图 5 为叶片振型图,叶片低阶振型较为简单,高阶振型复杂,一阶振型为挥舞振动,二阶振型为摆振振动,三阶和四阶振型为高次挥舞振动,五阶振型为挥舞-摆振耦合振动。叶片从第六阶振型出现明显的扭转现象,第六阶振型为 3 种振动的耦合。

与 0°铺层角度叶片相比,不同铺层角度下叶片固有频率的相对改变量如图 6 所示,叶片一阶、二阶和四阶固有频率的变化趋势相似,随着铺层角度增加,叶片固有频率逐渐减小。五阶固有频率下降趋势与上述 3 种固有频率相近,但铺层角度为 15°和 30°时,其固有频率略有增加。叶片三阶和六阶固有频率随铺层角度增加先增加后减小,铺层角度为 45°时,叶片固有频率达到最大。铺层角度增加对叶片的一阶、二阶、四阶和五阶振型影响较大,这是由于铺层角度导致叶片挥舞和摆振方向的等效刚度逐渐下降。叶片六阶振型出现扭转现象,适当增加铺层角度能提升叶片抗扭能力,因此其六阶固有频率有所增加。

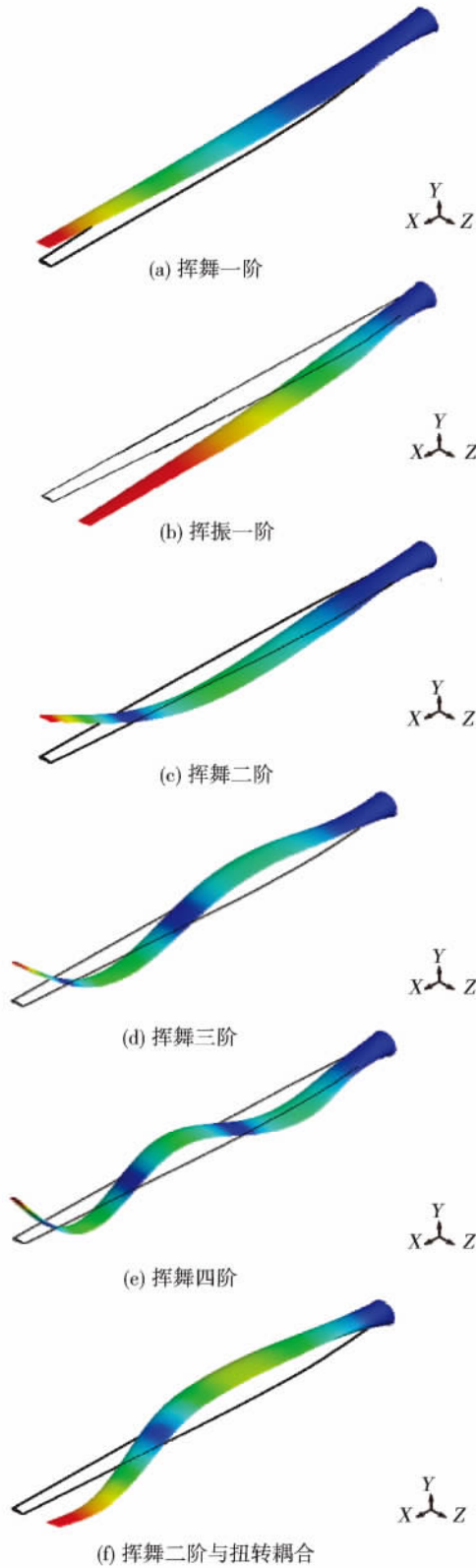


图5 叶片前六阶模态振型
Fig.5 First six order modals and vibration patterns of the blade

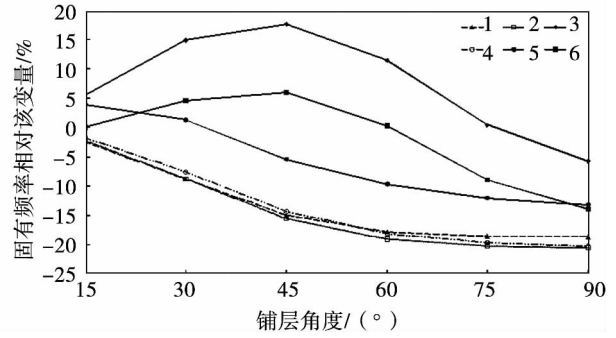


图6 不同角度铺层与0°铺层固有频率相对改变量

Fig.6 Comparison of natural frequency between blades with different ply angles and 0° ply angle

5 结论

本文采用复合材料建立多种层合板方案,实现1.5 MW 风力机叶片铺层,并基于有限元法,获得了不同铺层参数下叶片的动力学特性。通过对比多种铺层方案下叶片的模态可得出以下结论:

(1) 铺层角度是影响叶片固有频率的重要因素,复合材料具有显著正交各向异性,铺层角度改变引起叶片挥舞和摆振方向的刚度变化,从而影响固有频率大小,叶片固有频率具有可设计性;

(2) 叶片低阶振型主要以挥舞和摆振为主,铺层角度增加导致叶片这两个方向截面刚度下降,使叶片更易发生共振,因此需增加0°铺层比例;

(3) 叶片高阶模态出现扭转现象,铺设45°复合材料能提高叶片抗扭能力,增加叶片高阶模态固有频率。

参考文献:

[1] 李春,叶舟,高伟,等.现代大型风力机设计原理[M].上海:上海科学技术出版社,2013.
LI Chun ,YE Zhou ,GAO Wei ,et al. Modern large-scale wind turbine designprinciples[M]. Shanghai: Shanghai Science and Technology Press 2013.

[2] Sieros G ,Chaviaropoulos P ,Sørensen J D ,et al. Upscaling wind turbines: theoretical and practical aspects and their impact on the cost of energy [J]. Wind Energy 2012 ,15(1) : 3 -17.

[3] Skrzypiński W ,Gaunaa M. Wind turbine blade vibration at standstill conditions-the effect of imposing lag on the aerodynamic re-

- sponse of an elastically mounted airfoil [J]. *Wind Energy* 2015, 18(3): 515–527.
- [4] LIAO Cai-cai, ZHAO Xiao-lu, WANG Jian-li, et al. Optimization design of the frequency based on wind turbine blade layers [J]. *Journal of Engineering Thermophysics*, 2011, 32(8): 1311–1314.
- [5] 刘伟,尹家聪,陈璞,等.大型风力机复合材料叶片动态特性及气弹稳定性分析[J].*空气动力学学报* 2011, 29(3): 391–395.
LIU Wei, YIN Jia-cong, CHEN Pu, et al. Dynamic characteristics and aeroelastic stability analysis of the composite material-made blades of a wind turbine [J]. *Acta Aerodynamica Sinica* 2011, 29(3): 391–395.
- [6] Overgaard L C T, Lund E, Thomsen O T. Structural collapse of a wind turbine blade. Part A: Static test and equivalent single layered models [J]. *Composites Part A: Applied Science and Manufacturing* 2010, 41(2): 257–270.
- [7] 张旭,邢静忠.叶片局部损伤对大型水平轴风力机静态特性影响的仿真分析[J].*工程力学* 2012, 30(2): 406–412.
ZHANG Xu, XING Jing-zhong. Simulation analysis of the effect of a local damage to a blade on the static and dynamic characteristics of a large-sized horizontal shaft wind turbine [J]. *Engineering Mechanics* 2012, 30(2): 406–412.
- [8] Gangele A, Ahmed S. Modal analysis of S809 wind turbine blade considering different geometrical and material parameters [J]. *Journal of The Institution of Engineers* 2013, 94(3): 225–228.
- [9] Griffith D T, Carne T G. Experimental modal analysis of 9-meter research-sized wind turbine blades [M]. New York: Springer 2011.
- [10] 张兰挺,邓海龙,郝佳佳,等.铺层参数对风力机叶片静态结构性能的影响分析[J].*太阳能学报* 2014, 35(6): 023–029.
ZHANG Lan-ting, DENG Hai-long, GAO Jia-jia, et al. Analysis of the influence of the lamination layer parameters on the static structural performance of the blades of a wind turbine [J]. *Acta Energetica Solaris Sinica* 2014, 35(6): 023–029.
- [11] 梁利华,谢少军,潘柏松.铺层纤维方向对风力机叶片强度的影响分析[J].*太阳能学报* 2014, 35(5): 017–023.
LIANG Li-hua, XIE Shao-jun, PAN Bai-song. Analysis of the influence of the fabric direction in the lamination layer on the strength of blades in a wind turbine [J]. *Acta Energetica Solaris Sinica* 2014, 35(5): 017–023.
- [12] Zienkiewicz O C, Taylor R L, Zienkiewicz O C, et al. The finite element method [M]. London: McGraw-hill, 1977.
- [13] Gibson R F. Principles of composite material mechanics [M]. Boca Raton: CRC press 2011.
- [14] 陈余岳,张锦南.玻璃钢/复合材料风力机叶片的开发[J].*上海电力* 2007, 20(4): 371–374.
CHEN Yu-yue, ZHAN Jin-nan. Development of fiber reinforced plastics/composite material-made blades in wind turbines [J]. *Shanghai Electric Power* 2007, 20(4): 371–374.
- [15] 安利强,周邢银,赵鹤翔,等.5 MW 风力机叶片模态特性分析[J].*动力工程学报* 2013, 33(11): 890–894.
AN Li-qiang, ZHOU Xing-yin, ZHAO He-xiang, et al. Analysis of the modal characteristics of the blades in a 5 MW wind turbine [J]. *Journal of Power Engineering* 2013, 33(11): 890–894.
- [16] 刘旺玉,龚佳兴,刘希凤,等.基于弯扭耦合的自适应风力机叶片设计[J].*太阳能学报* 2011, 32(7): 1014–1019.
LIU Wang-yu, GONG Jia-xing, LIU Xi-feng, et al. Bowed-twisted-coupling-based self-adaptive design of blades in wind turbines [J]. *Acta Energetica Solaris Sinica* 2011, 32(7): 1014–1019.
- [17] 周鹏展,肖加余,曾竟成,等.基于 ANSYS 的大型复合材料风力机叶片结构分析[J].*国防科技大学学报* 2010, 32(2): 46–51.
ZHOU Peng-zhan, XIAO Jia-yu, ZENG Jing-cheng, et al. Analysis of the structure of the composite material-made blades in a large-sized wind turbine based on the software ANSYS [J]. *Journal of National University of Defense Technology*, 2010, 32(2): 46–51.
- [18] 靳交通,潘利剑,彭超义,等.风力机叶片截面弯曲刚度有限元分析方法[J].*太阳能学报* 2013, 34(2): 196–201.
JIN Jiao-tong, PAN Li-jian, PENG Chao-yi, et al. Method for finite element analyzing the bending stiffness of the blade in a section in a wind turbine [J]. *Acta Energetica Solaris Sinica* 2013, 34(2): 196–201.

(刘瑶 编辑)

Aerodynamic Performance of a Dual-section Type Airfoil [刊 汉]/QI Liang-kui ,LIU Jian-hua ,ZHANG Liang ,LIAO Yu-kai (College of Energy Source and Power Engineering ,Shanghai University of Science and Technology ,Shanghai ,China ,Post Code: 200093) ,LIU Jian-hua (Shanghai City Key Laboratory on Multi-phase Flow and Heat Transfer in Power Engineering ,Shanghai ,China ,Post Code: 200093) //Journal of Engineering for Thermal Energy & Power. -2016 31(9) . -45 ~ 51

With the Spalart-Allmaras(S-A) turbulent flow model serving as the calculation model ,a numerical simulation of the fluid flow conditions of the NACA0018 airfoil was performed under the condition of the swaying angle of the flap being 0 degree ,5 degrees ,10 degrees and 15 degrees respectively. In this connection ,the lifting drag performance curves of the airfoil provided with a flap ,contours of the distribution of the pressure on the surface of the airfoil and the flow field streamline chart at various attack angles were also analyzed and the influence of the swaying angle on the aerodynamic performance of the airfoil provided with a flap was studied. It has been found that at a same attack angle ,the lifting force coefficient of the airfoil will decrease with an increase of the swaying angle of the flap. To increase the swaying angle of the flap can increase the attack angle of the airfoil when it goes into a stall ,improve the flow conditions of the fluid around the airfoil ,enhance the flow stability of the fluid around the airfoil ,especially around the flap and contain the formation of the flow-separation-caused vortexes. **Key words:** flap ,swaying angle ,stall ,vortex

基于气动弹性剪裁的风力机叶片模态分析 = Analysis of the Modal of a Blade in a Wind Turbine Based on the Aeroelastic Tailoring [刊 汉]/CHEN Wen-pu ,LI Chun ,YE Zhou ,MIAO Wei-pao (College of Energy Source and Power Engineering ,Shanghai University of Science and Technology ,Shanghai ,China ,Post Code: 200093) ,LI Chun ,YE Zhou (Shanghai City Key Laboratory on Multi-phase Flow and Heat Transfer in Power Engineering ,Shanghai ,China ,Post Code: 200093) //Journal of Engineering for Thermal Energy & Power. -2016 31(9) . -52 ~ 57

To study the influence of the lamination parameters of a blade on its dynamic characteristics ,prevent the blade from any resonance and improve the characteristics of the blade in mechanics ,established was a finite element model for blades in a 1.5 MW wind turbine. Through changing the angle and the fiber proportion of the lamination layer ,the authors implemented a variety of the lamination layers of the blade in various ply plate structure and conducted an analysis of the modal of various lamination structures of the blade above mentioned ,obtained the first six order intrinsic frequencies and vibration patterns of various models and analyzed the causes of the lamination parameters influencing the dynamic characteristics of the blade. It has been found that the composite materials have their significant anisotropy and to change the angle of the lamination layer can influence the magnitude of the intrinsic frequency. The flapwise and edgewise vibration will dominate the low order vibration patterns of the blade and to increase the proportion of the lamination layers at an angle of 0 degree can enhance the low order intrinsic frequency and the torsional vibration will occur in the high order modal. The lamination layer at an angle of 45 degrees can enhance the torsion-resistant capacity of the blade and contribute to enhancing the high order intrinsic frequency. **Key**

words: wind turbine blade ,aeroelastic tailoring ,modal

700 °C 亚临界无再热发电机组技术的经济性分析 = **Analysis of the Cost-effectiveness of the 700 °C Subcritical Reheat-less Power Generation Unit Technology** [刊 ,汉] /QU Ke-nan ,YAN Wei-ping ,MENG Yan (College of Energy Source ,Power and Mechanical Engineering ,North China University of Electric Power ,Baoding ,China , Post Code: 071003) //Journal of Engineering for Thermal Energy & Power. -2016 31(9) . -58 ~62

When the steam temperature can not further increase ,to increase the main steam pressure and adopt a reheat cycle can enhance the thermal efficiency of the thermal cycle of a unit. However ,with an increase of the pressure ,the energy consumption rate of the feedwater pumps ,wall thickness of the pressure components and the investment in the metal materials will all increase by a great margin. A reheat system will not only make the initial investment increase substantially but also force the pressure loss of the system and the heat dissipation loss in the pipelines to increase and heighten the operation difficulty. When the main steam temperature attains a level of 700 °C ,under the precondition of the basic parameters being identical ,the cost-effectivenesses of a 18 MPa/720 °C 1 000 MW subcritical reheat-less natural cycle unit and a 35 MPa/700 °C /720 °C 1 000 MW ultra-supercritical primary reheat unit were analyzed and contrasted and the feasibility of designing a 700 °C subcritical reheat-less unit was also exploratorily investigated. The calculation results based on the Carnot cycle in the thermodynamics show that the heat rate of the steam turbine of a unit without any reheat will increase by 465.73 kJ/(kW · h) and the power supply coal consumption rate will increase by 13.15 g/(kW · h) when compared with those of a primary reheat unit. Such economic factors as the prices of Ni-base high temperature steel materials for use at or above 700 °C ,the unit price of standard coal ,loan interest rate and annual operation hours of the units etc. were taken into account in a comprehensive way and the balances of annual investment costs in both units converted in various numbers of years in operation were also compared. The comprehensive cost-effective analytic results show that the cost-effectiveness of the subcritical reheat-less unit in the number of years of the whole service life will be obviously superior to that of an ultra-supercritical primary reheat unit. **Key words:** 700 °C ,reheat-free ,thermal efficiency ,cost-effectiveness

链条锅炉复合燃烧炉内特性的数值模拟研究 = **Numerical Simulation and Study of the In-furnace Compound Combustion Characteristics of a Chain Grate Boiler** [刊 ,汉] /SAI Qing-yi ,YAN Hao-wen ,ZHANG Zhong-xiao (Shanghai University of Science and Technology ,Shanghai ,China ,Post Code: 200090) ,CHEN Bao-ming (Huazhibang Science and Technology Stock-holding Co. Ltd. ,Shanghai ,China ,Post Code: 200090) //Journal of Engineering for Thermal Energy & Power. -2016 31(9) . -63 ~68

With a 35 t/h chain grate boiler in a chemical plant serving as the physical model ,the CFD software Fluent was adopted to perform a numerical simulation and calculation of the characteristics of the speed field and temperature field in the furnace of a chain grate boiler before and after the reconstruction by using the compound combustion technology. The calculation results show that after the reconstruction by using the compound combustion technology ,